Constant-Spacing Connected Platoons With Robustness to Communication Delays

Yudong Lin, Anuj Tiwari, Brian Fabien, and Santosh Devasia, *Fellow, IEEE*

***Abstract*— This paper proposes an approach to make constant-spacing vehicle platoons robust to large delays and loss of communication. It is well known that centralized communication of the desired trajectory is important to simultaneously guarantee both string stability and constant-spacing in platoons. However, the performance of the resulting connected vehicle system (CVS) is vulnerable to large communication delays and communication loss. The main contribution of this work is a new delayed-self-reinforcement-based (DSR-based) approach that approximates the centralized communication based control by a decentralized predecessor follower (PF) control. The resulting blending of centralized communication with the decentralized DSR approach results in predecessor-leader follower (PLF) control with (i) robustness of the convergence to consensus under large communication delays and (ii) substantially-smaller spacing errors under loss of communication. Comparative simulations show that, for the same level of robustness to internal-stability and string-stability, the variation in settling time to consensus for PLF with DSR under large communication delays is 95% less than PLF without DSR and the steady-state error with DSR under loss of communication is 80% less than PLF without DSR.**

***Index Terms*— Vehicle platoon, consensus, string stability, delays, communication loss.**

I. Introduction

LONGITUDINAL cruise control with constant spacing policy (CSP) enables platoons with small inter-vehicle distances, resulting in improved fuel efficiency, and increased traffic throughput [1], [2], [3]. However, it is well-known that constant spacing cannot be maintained together with string stability when using decentralized predecessor-follower (PF) methods, which rely only on local sensing information about the preceding vehicle [4], [5]. Predecessor-leader-follower (PLF), with centralized communication from the leader vehicle to the followers, resolves the problem and enables constant spacing with string stability [6], [7]. However, the performance of the resulting connected vehicle system (CVS) is vulnerable to communication issues [8], e.g. (i) large communication delays can lead to slower oscillatory convergence to consensus and and (ii) communication loss can lead to large spacing errors. Large communication delay and communication loss can be caused by environmental jamming or during transmission over long distances. For example, in locations with high rate of jamming, the system needs to reduce the packet delivery rate in order to reject unwanted messages [9]. Furthermore, large transmission and receiving distances in the hundreds of meters, which is anticipated for truck platooning on highways, can greatly increase the path loss and communication delay of vehicle to vehicle communication [10]. Therefore, there is a need to develop PLF protocols with robust performance in the presence of such communication problems.

Previous works have addressed the issue of small communication delays or short periods of communication loss on the performance of the connected vehicle system (CVS). For example, an upper bound of communication delay to maintain string stability depends on the vehicle dynamics and can be found numerically [11] or analytically depending on the selected headway time [12]. Furthermore, sufficient conditions on the communication delay can be derived analytically to guarantee the internal stability [13] and string stability [7]. However, for large communication delays, even with string stability and internal stability, the performance in terms of settling time (for converging to consensus) can be large. Similarly, short term communication loss can be addressed using estimation techniques to infer the lost centralized command [14], [15], [16]. However, such methods are not applicable for large delays in communication or when communication is lost for long periods of time. In particular, when the communication is lost for extended periods of time, the PLF structure degrades to the PF structure with only the decentralized protocol, which cannot maintain both constant spacing and string stability as discussed before. Thus, current CSP has challenges when dealing with large communication delays or loss in communication for extended periods of time.

The current work develops a PLF protocol that (i) enlarges the acceptable upper bound of communication delays for maintaining string stability and constant spacing, and (ii) reduces the constant spacing error when CVS degrades to PF protocol due to communication loss. The main idea is to use the delayed self reinforcement (DSR) approach [17] for the decentralized part of the PLF. The DSR approach seeks to implement the ideal, non-delayed centralized command which results in ideal platooning from the current and delayed local sensing information, and to improved cohesion. Since the DSR approximates the ideal centralized command, it leads to low spacing errors in the platoon with large communication delays and even

Manuscript received 1 April 2022; revised 31 August 2022; accepted 21 November 2022. Date of publication 9 February 2023; date of current version 1 March 2023. The Associate Editor for this article was L. Du. *(Corresponding author: Santosh Devasia.)*

Yudong Lin, Anuj Tiwari, and Santosh Devasia are with the Department of Mechanical Engineering, University of Washington, Seattle, WA 98195 USA (e-mail: yudong17@uw.edu; anujt@uw.edu; devasia@uw.edu).

Brian Fabien is with the Department of Mechanical Engineering, University of Portland, Portland, OR 97203 USA (e-mail: fabien@up.edu).

Digital Object Identifier 10.1109/TITS.2022.3224635

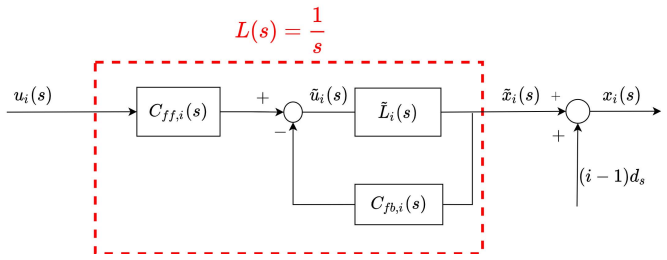

Fig. 1. Stable pole-zero cancellations using controllers $C_{ff,i}$, $C_{fb,i}$ in Eqs. (3), (4) reduces the vehicle dynamics $\tilde{L}_i$ to a single-integrator system L depicted inside the red dashed box. x_i is the deviation from the ideal spacing $(i-1)d_s$ with respect to the lead vehicle, as in Eq. (10).

when the communication is lost. The main contributions of the current work are the following.

(i) Development of a new blended PLF with both (a) decentralized DSR and (b) centralized communication as opposed to purely decentralized case studied in prior work [17].

(ii) Finding conditions for the blended DSR-based, constant-spacing PLF to guarantee internal stability and string stability with delayed centralized command and loss of communication. Moreover, the steady state spacing error under communication loss is also quantified.

(iii) Illustration of the DSR parameter selection and impact under different communication conditions using a simulation example.

II. Problem Formulation

A. Individual Vehicle Dynamics

Each vehicle's input-to-output dynamics can be made homogeneous using input-output feedback linearization even if the original dynamics is heterogeneous and nonlinear, e.g., as in [18] and [19] to obtain in the Laplace domain

$$\tilde{L}_i(s) = \frac{\tilde{x}_i(s)}{\tilde{u}_i(s)} = \frac{1}{s^{m_i}}, \tag{1}$$

where $\tilde{x}_i \in \mathbb{R}$ and $\tilde{u}_i \in \mathbb{R}$ are the output position and input of i^{th} vehicle in the system, and m_i is the relative degree. Stable pole-zero cancellation is achieved by selecting the control law

$$\tilde{u}_i(s) = C_{ff,i}(s)u_i(s) - C_{fb,i}(s)\tilde{x}_i(s) \tag{2}$$

as in Fig. 1 with feedback controllers $C_{ff,i}, C_{fb,i}$

$$C_{ff,i}(s) = s^{m_i-1} + k_1 s^{m_i-2} + \cdots + k_{m_i-1}, \tag{3}$$
$$C_{fb,i}(s) = k_1 s^{m_i-1} + k_2 s^{m_i-2} + \ldots k_{m_i-1}s, \tag{4}$$

resulting in a first-order closed-loop dynamics $L_i(s)$

$$\begin{aligned} L_i(s) = \frac{\tilde{x}_i(s)}{u_i(s)} &= \frac{\tilde{L}_i(s)C_{ff,i}(s)}{1+\tilde{L}_i(s)C_{fb,i}(s)} \\ &= \frac{(s^{m_i-1} + k_1 s^{m_i-2} + k_2 s^{m_i-3} + \ldots k_{m_i-1})}{s(s^{m_i-1} + k_1 s^{m_i-2} + k_2 s^{m_i-3} + \ldots k_{m_i-1})} \\ &= \frac{1}{s} = L(s). \end{aligned} \tag{5}$$

The controller gains $k_1, \ldots, k_{m_i-1}$ are designed to avoid unstable pole-zero cancellations by ensuring that the cancelled polynomial $p_i(s) = s^{m_i-1} + k_1 s^{m_i-2} + \cdots + k_{m_i-1}$ has roots in the open left-half of the complex-plane. For example, if each individual vehicle dynamics is a second-integrator model $\tilde{L}_i(s) = s^{-2}$ as in [19] and [7], then the controllers

$$C_{ff,i}(s) = s + k_1, \qquad C_{fb,i}(s) = k_1 s, \tag{6}$$

with $k_1 > 0$, would achieve the reduction to the single-integrator system in Eq. (5).

B. Ideal Centralized CSP

To maintain constant spacing in a platoon, an ideal scenario is for each vehicle i in the set of positive integers $\mathcal{N}$, i.e., $i \in \mathcal{N}$ to receive information about its desired position $\tilde{x}_{d,i}$ from a virtual source as

$$\tilde{x}_{d,i}(t) = x_0(t) - (i-1)d_s, \tag{7}$$

where x_0 is the desired position of the lead vehicle $i = 1$ and d_s is the desired spacing between adjacent vehicles. Then, each vehicle in the platoon applies the control law

$$u_i(t) = -\alpha(\tilde{x}_i(t) - \tilde{x}_{d,i}(t)), \tag{8}$$

and $\alpha > 0$ defines the time constant $1/\alpha$. The resulting dynamics can be written as, from Eqs. (5) and (8),

$$\dot{x}_i(t) = -\alpha x_i(t) + \alpha x_0(t) \quad = u_{c,i}(t), \tag{9}$$

where the position x_i is defined as the deviation from the ideal spacing with respect to the lead vehicle, i.e.,

$$x_i(t) = \tilde{x}_i(t) - (-(i-1)d_s) = \tilde{x}_i(t) + (i-1)d_s. \tag{10}$$

It is assumed that all vehicles have the desired spacing initially, i.e., $x_i(0) = x_0(0)$ for all $i \in \mathcal{N}$. With the ideal centralized input $u_{c,i}$ in Eq. (9), all vehicle responses are the same, i.e., $x_i(t) = x_j(t)$, and therefore, the constant-spacing policy (CSP) can be maintained for a given desired position trajectory x_0. In matrix form, the ideal centralized control in Eq. (9) can be written as

$$\dot{X}(t) = -\alpha \mathbf{I} X(t) + \alpha \mathbf{1} x_0(t) \ = u_c(t), \tag{11}$$

where $X = [x_1, x_2, \ldots, x_n]^T$, $\mathbf{I}$ is the $n \times n$ identity matrix, and $\mathbf{1}$ is an $n \times 1$ vector of ones.

C. Decentralized CSP With Delayed Self Reinforcement

The ideal centralized approach in Eq. (11) can be approximated to be decentralized (e.g., where only the lead vehicle has access to the desired trajectory x_0) using the delayed self reinforcement (DSR) approach in [17], as described below. Multiplying Eq. (11) with βK, where β is the DSR gain and K is the pinned graph Laplacian of the CVS network without the virtual source, with nonzero off-diagonal elements $K_{i,j} = -1$ only if vehicle i receives information (through sensing or communication) about vehicle j where $i \neq j$, and the diagonal elements are $K_{i,i} = B_i - \sum_j K_{i,j}$ with nonzero $B_i = 1$ only if vehicle i receives information about the desired position x_0 from the virtual source $i = 0$, the ideal centralized dynamics can be rewritten as

$$\beta K \dot{X}(t) = -\alpha\beta K X(t) + \alpha\beta K \mathbf{1} x_0(t). \tag{12}$$

If the CVS connectivity contains information paths from the virtual source node $i = 0$ (providing the desired position information) to each vehicle in the platoon, then the pinned Laplacian K of the graph without the source node $i = 0$ is invertible, i.e., $\det(K) \neq 0$ from the Matrix-Tree Theorem in [20]. Moreover, the vehicles will achieve consensus eventually, i.e., $K^{-1}B = \mathbf{1}$, where B is the source connectivity vector (i.e. row element is nonzero $B_i = 1$ only if vehicle i is connected to the source and is zero otherwise). Finally, adding $\dot{X}(t)$ on both sides of Eq. (12) and rearranging, results in

$$\dot{X}(t) = (\mathbf{I} - \beta K)\dot{X}(t) - \alpha\beta K X(t) + \alpha\beta B x_0(t). \quad (13)$$

The DSR approach [17] uses delayed versions of already available information to implement the derivative on the right hand side of Eq. (13) as

$$\begin{aligned}\dot{X}(t) &= (\mathbf{I} - \beta K)\frac{X(t) - X(t-\tau_d)}{\tau_d} \\ &\quad - \alpha\beta K X(t) + \alpha\beta B x_0(t), \\ &= u_{dsr}(t). \end{aligned} \quad (14)$$

The above DSR approach can be implemented in a decentralized manner, e.g., with source information available only to the leader vehicle, and it approximates the performance of the centralized approach when the desired trajectories vary slowly compared to the time delay $\tau_d > 0$ in Eq. (14). Conditions for stability in terms of the DSR gain β and delay τ_d have been established in [17].

Remark 1 (DSR implementation): An advantage of the DSR approach is that it does not require additional sensing or communication. Rather, current and delayed versions of the sensed signals KX and the vehicles position x_i, already available to the vehicle controller, are sufficient for implementation.

Remark 2 (DSR for higher-order vehicle dynamics): The DSR approach to decentralize the ideal cohesive dynamics as in Eq. (14) can be applied even if the homogeneous dynamics L in Eq. (5) of the vehicle is higher order [17].

D. Problem Statement

In this article, we consider the blending of the centralized and decentralized DSR approach to achieve good performance even when communication about the desired trajectory x_0 is not always available for all the vehicles. With the blended approach, from Eqs. (11) and (14),

$$\begin{aligned}\dot{x}_i(t) &= \gamma\, u_{dsr,i}(t-\tau_l) + (1-\gamma)u_{c,i}(t-\tau_c), \quad \forall i \geq 2 \\ \dot{x}_1(t) &= \gamma\, u_{dsr,1}(t-\tau_l) + (1-\gamma)u_{c,1}(t-\tau_l), \end{aligned} \quad (15)$$

where $0 \leq \gamma \leq 1$ is the blending gain, $\tau_c > 0$ is the communication delay, $\tau_l > 0$ is the local sensing delay, and, $u_{dsr,i}$ and $u_{c,i}$ are the i^{th} elements of the DSR and centralized control inputs respectively. Since the leader has the source information x_0, the local sensing delay τ_l is applied instead of the communication delay τ_c in Eq. (15). The blended approach Eq. (15) is referred to as PLF with DSR in the following.

Remark 3 (Small communication delay to the leader): Typically, the leader can compute and generate the source trajectory locally before broadcasting to the followers [21]. Therefore, the communication delay of the leader to the source trajectory is assumed to be small, and is considered to be the same as the local sensing delay τ_l.

Remark 4 (Homogeneous time delays): The time delays τ_c, τ_l, τ_d can be varying for each vehicle. However, they are assumed to be the same for all vehicles to promote cohesive responses. If the actual delays are different, each vehicle can add intentional buffer delays (as needed) to maintain homogeneity in the delays for all vehicles as in Ref. [7].

The following three research questions are addressed next.

(1) Internal stability of CVS: What are the conditions on the blended protocol in Eq. (15) to ensure internal stability of the CVS, i.e., for the real parts of the poles of the individual-vehicle transfer functions

$$T_i(s) = \frac{x_i(s)}{x_0(s)} \quad (16)$$

to be negative?

(2) String stability: What are the conditions on the blended protocol in Eq. (15) to guarantee string stability of the CVS? The CVS is said to be string stable if the spacing errors do not amplify along the vehicle platoon downstream, i.e. the magnitudes of the error propagation transfer functions $G_i(s)$ of the followers ($i \geq 2$) satisfy

$$\left| G_i(j\omega) = \frac{\delta_{i+1}(s)}{\delta_i(s)} \right| < 1, \qquad \forall \omega > 0, \quad (17)$$

where the spacing error δ_i defined as

$$\delta_i(s) = x_{i-1}(s) - x_i(s). \quad (18)$$

(3) Steady-state error: Does the steady-state error converge to zero under the blended protocol in Eq. (15)? Given a step change in the desired velocity, i.e. $v_0(s) = V/s$, the CVS has no steady state error if the spacing error δ_i in Eq. (18) converges to zero for all vehicles, i.e.,

$$\lim_{t\to\infty} \delta_i(t) = \lim_{s\to 0} s\delta_i(s) = 0 \qquad \forall i \in \mathcal{N}. \quad (19)$$

III. Analysis of Blended DSR for PLF Networks

Internal stability, string stability and steady-state errors for the CVS are established in this section.

A. Internal Stability of CVS

Conditions for internal stability of the CVS are developed by (i) finding the transfer functions T_i in Eq. (16) of the vehicle responses x_i to the desired lead vehicle position x_0, and then (ii) finding requirements to ensure that the poles of the transfer functions T_i are on the open left half of the complex plane.

1) Dynamics of the Vehicles: Each vehicle uses both the relative positioning error (with respect to the predecessor) and the source positioning error in control, as illustrated in Fig. 2 with the predecessor leader follower network, where the associated pinned graph Laplacian $K \in \mathbb{R}^{n\times n}$ in Eq. (14) and the source connectivity vector $B \in \mathbb{R}^n$ are given by [22]

$$K = \begin{bmatrix} 1 & \dots & & 0 \\ -1 & 1 & & \\ \vdots & \ddots & \ddots & \\ 0 & \dots & -1 & 1 \end{bmatrix}, \quad B = \begin{bmatrix} 1 \\ 0 \\ \vdots \\ 0 \end{bmatrix}. \quad (20)$$

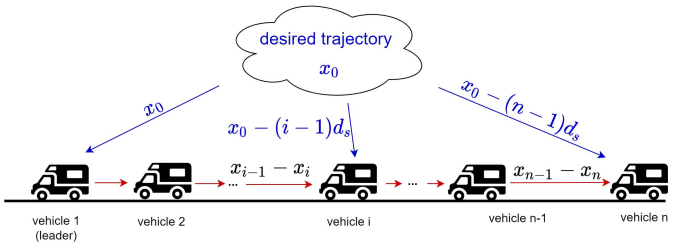

Fig. 2. Predecessor-Leader-Follower (PLF) vehicle platoon with n vehicles. Each follower vehicle $i \geq 2$ gets (i) centralized information about its desired position $\tilde{x}_{d,i} = x_0(t) - (i-1)d_s$ in Eq. (7) where x_0 is the desired position of the lead vehicle and (ii) decentralized local sensing information of its own position x_i in Eq. (10) and the relative positioning error $\delta_i = x_{i-1} - x_i$ in Eq. (18) with respect to its predecessor vehicle.

The leader ($i = 1$) vehicle's state equation with the DSR approach (Eq. (14)), for the pinned graph Laplacian K and source connectivity vector B as defined in Eq. (20), is found to be,

$$\begin{aligned}\dot{x}_1(t) &= (1-\beta)\frac{x_1(t) - x_1(t-\tau_d)}{\tau_d} - \alpha\beta\,(x_1(t) - x_0(t)) \\ &= u_{dsr,1}(t),\end{aligned} \tag{21}$$

and the state equation for the followers $i > 1$ is obtained as,

$$\begin{aligned}\dot{x}_i(t) = (1-\beta)\frac{x_i(t) - x_i(t-\tau_d)}{\tau_d} + \beta\frac{x_{i-1}(t) - x_{i-1}(t-\tau_d)}{\tau_d} \\ - \alpha\beta(x_i(t) - x_{i-1}(t)) \quad = u_{dsr,i}(t).\end{aligned} \tag{22}$$

The dynamics of the i^{th} vehicle $\dot{x}_i(t)$ can be found by substituting the DSR command from Eqs. (21), (22) and the centralized command from Eq. (11) into the blended protocol in Eq. (15) to obtain, in the Laplace domain,

for $i = 1$,

$$\frac{x_1(s)}{x_0(s)} = \frac{G_{c0}(s)}{s-(1-\beta)G_m(s)+G_{c0}(s)} = \frac{G_{c0}(s)}{D_0(s)} = T_1(s), \tag{23}$$

where $T_1(s)$ is the position-transfer function for the lead vehicle, and for the follower vehicles, $i \geq 2$,

$$\begin{aligned}x_i(s) &= \frac{G_c(s)x_0 + G_f(s)x_{i-1}}{s - G_m(s) + G_f(s) + G_c(s)} \\ &= \frac{G_c(s)x_0 + G_f(s)x_{i-1}}{D(s)},\end{aligned} \tag{24}$$

with

$$G_m(s) = \gamma\, e^{-s\tau_l}\frac{1 - e^{-s\tau_d}}{\tau_d}, \tag{25}$$

$$G_f(s) = \beta\gamma\, e^{-s\tau_l}(\alpha + \frac{1 - e^{-s\tau_d}}{\tau_d}), \tag{26}$$

$$G_{c0}(s) = \alpha(1 - \gamma\,(1-\beta))e^{-s\tau_l}, \tag{27}$$

$$G_c(s) = \alpha(1-\gamma)e^{-s\tau_c}, \tag{28}$$

$$D_0(s) = s - (1-\beta)G_m(s) + G_{c0}, \tag{29}$$

$$D(s) = s - G_m(s) + G_f(s) + G_c(s). \tag{30}$$

Lemma 1: The position transfer functions $T_i(s)$ in (16) for the follower vehicles $i \geq 2$ are given by

$$T_i(s) = \left[\frac{G_c(s)}{D(s)}\sum_{j=0}^{i-2}\left(\frac{G_f(s)}{D(s)}\right)^j\right] + \left(\frac{G_f(s)}{D(s)}\right)^{i-1} T_1(s), \tag{31}$$

where $T_1(s)$ is the lead-vehicle transfer function in Eq. (23).

Proof: Eq. (31) can be shown by induction

1) Base case ($i = 2$): The position transfer function $T_2(s)$ can be computed from Eqs. (23) and (24) as

$$T_2(s) = \frac{G_c(s)}{D(s)} + \frac{G_f(s)}{D(s)}T_1(s), \tag{32}$$

which is equal to Eq. (31) with $i = 2$.

2) Induction step: Assume Eq. (31) is true when $i = k \geq 2$. Then, from Eq. (24)

$$T_{k+1}(s) = \frac{G_c(s) + G_f(s)T_k(s)}{D(s)}, \tag{33}$$

and using Eq. (31) for $T_k(s)$ results in

$$\begin{aligned}T_{k+1}(s) = \frac{G_c(s)}{D(s)} + \frac{G_f(s)}{D(s)}\left(\frac{G_c(s)}{D(s)}\sum_{j=0}^{k-2}\left(\frac{G_f(s)}{D(s)}\right)^j\right) \\ + \left(\frac{G_f(s)}{D(s)}\right)^k T_1(s) \\ = \frac{G_c(s)}{D(s)}\sum_{j=0}^{k-1}\left(\frac{G_f(s)}{D(s)}\right)^j + \left(\frac{G_f(s)}{D(s)}\right)^k T_1(s),\end{aligned} \tag{34}$$

which is equivalent to Eq. (31) with $i = k+1$.

□

2) Internal Stability Conditions: The following lemma shows that the CVS can be made internally stable if the delays in the vehicle control are small compared to the CVS time constant.

Lemma 2: The internal stability of the CVS protocol is independent of the DSR delay τ_d if the DSR gain β is selected as

$$\beta = 1. \tag{35}$$

Moreover, with this DSR-gain selection, the CVS with the blended protocol in Eq. (15) can always be stabilized if the local sensing delay τ_l and the communication delay τ_c are small compared to the CVS time constant $1/\alpha$,

$$\max\{\tau_l, \tau_c\} < \tfrac{\pi}{2}\left(\tfrac{1}{\alpha}\right). \tag{36}$$

Proof: The poles $s \in \mathbb{C}$ of the transfer functions T_1 in Eq. (23) and $T_i(s)$ in Eq. (31) correspond to the roots of $D_0(s) = 0$ and $D(s) = 0$. Then, substituting from Eqs. (25)-(28) into Eqs. (29) and (30) and using the condition $\beta = 1$ results in

$$D_0(s) = \quad s + \alpha e^{-s\tau_l} \quad = 0, \tag{37}$$

$$D(s) = \quad s + \alpha(\gamma\, e^{-s\tau_l} + (1-\gamma)e^{-s\tau_c}) \quad = 0. \tag{38}$$

The CVS is stable with poles (i.e., roots of Eqs. (37), (38)) at $s = -\alpha$ when the local sensing delay τ_l and the communication delay τ_c are zero and $\alpha > 0$. Therefore, from continuity of roots with parameter variations, the CVS will remain stable provided there is no imaginary axis crossing,

i.e., there is no frequency ω such that Eq. (37) or Eq. (38) is satisfied at $s = j\omega$ with $j = \sqrt{-1}$, i.e.,

$$\begin{aligned} D_0(j\omega) &= j\omega + \alpha e^{-j\omega\tau_l} \\ &= j\omega + \alpha[\cos(\tau_l\omega) - j\sin(\tau_l\omega)] = 0, \qquad (39) \\ D(j\omega) &= j\omega + \alpha(\gamma e^{-j\omega\tau_l} + (1-\gamma)e^{-j\omega\tau_c}) \\ &= \alpha(\gamma\cos(\tau_l\omega) + (1-\gamma)\cos(\tau_c\omega)) \\ &\quad + j(\omega - \alpha\gamma\sin(\tau_l\omega) - \alpha(1-\gamma)\sin(\tau_c\omega)) \\ &= 0. \qquad (40) \end{aligned}$$

which are known as D-curves in the D-subdivision method [23]. First, conditions are found for $D_o(j\omega) = 0$ to not have imaginary axis roots. Equating, the real and imaginary parts of $D_o(j\omega)$ to zero results in, from Eq. (39)

$$\alpha\cos(\tau_l\omega) = 0, \qquad (41)$$

$$\omega - \alpha\sin(\tau_l\omega) = 0. \qquad (42)$$

Eq. (41) is satisfied if

$$\tau_l\omega = \frac{\pi}{2} + n\pi, \qquad (43)$$

for $n \in \{0, 1, 2, 3, \ldots\}$, which when substituted in Eq. (42) identifies the (positive) imaginary-axis crossing frequency as $\omega^* = \alpha$, and the corresponding local sensing delays leading to imaginary-axis-crossing at $\omega^* = \alpha$, from Eq. (43), is

$$\tau_l^* = \frac{\pi}{2\alpha} + n\pi. \qquad (44)$$

Therefore, the imaginary axis crossing can be avoided if the the local sensing delay τ_l is smaller than the smallest τ_l^* value in Eq. (44) $\tau_l^* = \pi/(2\alpha)$, which leads to Eq. (36) of the current lemma.

Second, conditions are found for $D(j\omega) = 0$ to not have imaginary axis roots through the following three steps.

(i) There are no imaginary axis roots when $|\omega| > \alpha$. Equating the real and imaginary parts of $D(j\omega)$ to zero results in, from Eq. (40)

$$\alpha(\gamma\cos(\tau_l\omega) + (1-\gamma)\cos(\tau_c\omega)) = 0, \qquad (45)$$

$$\alpha(\gamma\sin(\tau_l\omega) + (1-\gamma)\sin(\tau_c\omega)) = \omega. \qquad (46)$$

Any solution ω satisfying Eq. (46) is bounded by α in magnitude, for $\gamma \in [0, 1]$, as shown below,

$$\omega = \alpha(\gamma\sin(\tau_l\omega) + (1-\gamma)\sin(\tau_c\omega)) \in [-\alpha, \alpha], \qquad (47)$$

since,

$$\begin{aligned} -1 &= \gamma(-1) + (1-\gamma)(-1) \\ &\le \gamma\sin(\tau_l\omega) + (1-\gamma)\sin(\tau_c\omega) \\ &\le \gamma + (1-\gamma) = 1. \qquad (48) \end{aligned}$$

Therefore, there can be no roots outside $[-\alpha, \alpha]$.

(ii) If there is an imaginary-axis crossing with $\omega \in [0, \alpha]$, then $-\omega$ would also be a solution since

$$\begin{aligned} &\alpha(\gamma\cos(-\tau_l\omega) + (1-\gamma)\cos(-\tau_c\omega)) \\ &\quad = \alpha(\gamma\cos(\tau_l\omega) + (1-\gamma)\cos(\tau_c\omega)) = 0, \qquad (49) \\ &\alpha(\gamma\sin(-\omega\tau_l) + (1-\gamma)\sin(-\omega\tau_c)) \\ &\quad = -\alpha(\gamma\sin(\omega\tau_l) + (1-\gamma)\sin(\omega\tau_c)) = -\omega. \qquad (50) \end{aligned}$$

(iii) There are no imaginary axis roots with $\omega \in [0, \alpha]$. Assume that there exists $\omega \in [0, \alpha]$ such that Eq.(45) is satisfied. Then,

$$\alpha(\gamma\cos(\tau_l\omega) + (1-\gamma)\cos(\tau_c\omega)) = 0. \qquad (51)$$

However, both cosine terms are positive, i.e., $\cos(\tau_l\omega) > 0$ and $\cos(\tau_c\omega) > 0$ since $\tau_l\omega \in [0, \frac{\pi}{2})$ and $\tau_c\omega \in [0, \frac{\pi}{2})$ when $\omega \in [0, \alpha]$ from the condition in Eq. (36) of the lemma. Therefore, the positively weighted sum of the cosines cannot be zero, and therefore,

$$\alpha(\gamma\cos(\tau_l\omega) + (1-\gamma)\cos(\tau_c\omega)) > 0, \qquad (52)$$

which contradicts the assumption that there exists $\omega \in [0, \alpha]$ that satisfies Eq. (45). Therefore, there is no imaginary axis crossing of the poles under the condition in Eq.(36) of the lemma, resulting in internal stability of the CVS. □

Internal stability is guaranteed when both the local sensing delay τ_l and the communication delay τ_c are bounded as in Eq. (36) of Lemma 2. For larger communication delays, the internal stability of CVS can still be guaranteed by using a sufficiently-large blending gain γ , as shown in the next lemma.

Lemma 3: The CVS with the blended protocol in Eq. (15) is internally stable, for any communication delay τ_c, if the local sensing delay τ_l and the blending gain γ satisfy

$$\tau_l < \frac{\pi}{2\alpha}, \qquad (53)$$

$$\frac{1}{1+\cos(\tau_l\alpha)} < \gamma \le 1 \qquad (54)$$

with the DSR gain $\beta = 1$ as in Remark 6.

Proof: Internal stability of the lead vehicle is established from Eq. (44) in the proof of Lemma 2, since the condition $\tau_l < \pi/(2\alpha)$ guarantees that there is no frequency $\omega \in \mathbb{R}$ such that $D_0(j\omega) = 0$ (Eq. (39)) is satisfied. For the followers, internal stability can be examined by judging whether there exists $\omega \in \mathbb{R}$ such that Eq. (45) and (46) are satisfied. With the blending gain γ selection as in Eq. (54), there is no $\omega \in [0, \alpha]$ that satisfies Eq. (45) since

$$\begin{aligned} &\alpha(\gamma\cos(\tau_l\omega) + (1-\gamma)\cos(\tau_c\omega)) \\ &\quad \ge \alpha(\gamma\cos(\tau_l\omega) - (1-\gamma)) \\ &\quad \ge \alpha((\cos(\tau_l\alpha)+1)\gamma - 1) > \alpha(1-1) = 0. \qquad (55) \end{aligned}$$

The second inequality in Eq.(55) follows since $\cos(\tau_l\omega)$ monotonically decreases on $\omega \in [0, \alpha]$, and $\tau_l\omega \le \tau_l\alpha < \pi/2$, from Eq. (53). Besides, using arguments in Steps 1 and 2 in the proof of Lemma 2, there can be no imaginary axis crossing when the frequency is large, $\omega > \alpha$ or negative, $\omega \le 0$. Thus, there is no imaginary axis crossing under the conditions of the lemma, resulting in internal stability of the CVS. □

Remark 5 (Blending gain selection): The CVS is internally stable for any selection of the blending gain $\gamma \in [0, 1]$ if the communication delay τ_c and local-sensing delays τ_l are small with respect to the time constant $1/\alpha$, i.e., smaller than $\pi/(2\alpha)$, according to Lemma 2. In the presence of large communication delay τ_c with respect to the time constant $1/\alpha$, i.e., $\tau_c \ge \pi/(2\alpha)$, sufficient use of the DSR input u_{dsr} (with a sufficiently-large blending gain as in Eq. (54)) also ensures internal stability.

Remark 6 (Internal stability assumption): The CVS is assumed to be internally stable in the rest of the article by satisfying the stability conditions of either Lemma 2 or Lemma 3 – including, $\beta = 1$.

B. String Stability of CVS

This section begins by finding the error propagation transfer functions $G_i(s)$, using which the conditions for string stability are established.

1) Error Dynamics of CVS: To assess string stability, the error propagation transfer functions $G_i, \forall i \in \mathcal{N}$ are obtained using the definition of the spacing error in Eq. (18) and the position transfer functions T_i in Eq. (16), as for $i = 1$,

$$G_1(s) = \frac{x_1(s) - x_2(s)}{x_0(s) - x_1(s)} = \frac{T_1(s) - T_2(s)}{1 - T_1(s)}, \tag{56}$$

and for $i \geq 2$,

$$G_i(s) = \frac{x_i(s) - x_{i+1}(s)}{x_{i-1}(s) - x_i(s)} = \frac{T_i(s) - T_{i+1}(s)}{T_{i-1}(s) - T_i(s)}. \tag{57}$$

The following existence lemma shows that the CVS can be made string stable if the delays in the vehicle control are small.

Lemma 4: The CVS, with the blended protocol in Eq. (15) satisfying the internal stability conditions as in Remark 6, meets the string stability condition in Eq. (17) on the error-propagation transfer function $G_i(s)$ provided the time delays in local sensing τ_l, communication τ_c and DSR τ_d are sufficiently small compared to the time constant $1/\alpha$ of the CVS, and the blending gain is less than one

$$\gamma < 1. \tag{58}$$

Proof: The approach is to find the error transfer function G_i in Eq. (57) and then find conditions to bound it to be less than one in three main steps. First, for all the follower vehicles ($i \geq 2$), the difference in the position transfer functions T_i can be found from Eq. (31) as

$$\begin{aligned} T_{i-1} - T_i &= \frac{G_c(s)}{D(s)} \left(\sum_{j=0}^{i-3} \left(\frac{G_f(s)}{D(s)} \right)^j - \sum_{j=0}^{i-2} \left(\frac{G_f(s)}{D(s)} \right)^j \right) \\ &\quad + T_1(s) \left(\left(\frac{G_f(s)}{D(s)} \right)^{i-2} - \left(\frac{G_f(s)}{D(s)} \right)^{i-1} \right) \\ &= \left(\frac{G_f(s)}{D(s)} \right)^{i-2} \left(\frac{G_c(s)}{D(s)} + T_1(s) \left(1 - \frac{G_f(s)}{D(s)} \right) \right), \end{aligned} \tag{59}$$

and since only the first term relates to the order of the vehicle i, the error transfer function in Eq. (57) becomes, for $i \geq 2$,

$$G_i(s) = \frac{T_i(s) - T_{i+1}(s)}{T_{i-1}(s) - T_i(s)} = \frac{G_f(s)}{D(s)}. \tag{60}$$

Second, the error transfer function G_i can be found by replacing G_f and D from Eq. (29) and Eqs. (25)-(28) with $\beta = 1$, as

$$G_i(s) = \frac{e^{-s\tau_l}\gamma\,(\alpha\tau_d + 1 - e^{-s\tau_d})}{\tau_d(s + \alpha(\gamma\, e^{-s\tau_l} + (1-\gamma)e^{-s\tau_c}))} = G(s), \tag{61}$$

which is independent of the vehicle number i. Third, from Eqs. (17) and (61), the string stability condition is

$$|G(j\omega)| = \left| \frac{e^{-j\omega\tau_l}\gamma\,(\alpha\tau_d + 1 - e^{-j\omega\tau_d})}{\tau_d(j\omega + \alpha(\gamma\, e^{-j\omega\tau_l} + (1-\gamma)e^{-j\omega\tau_c}))} \right| < 1,$$

for all $\omega > 0$, which is equivalent to (by squaring both sides and multiplying the denominator)

$$\begin{aligned} f(\omega, \gamma, \tau_c) &= \left| \tau_d(j\omega + \alpha(\gamma\, e^{-j\omega\tau_l} + (1-\gamma)e^{-j\omega\tau_c})) \right|^2 \\ &\quad - \left| e^{-j\omega\tau_l}\gamma\,(\alpha\tau_d + 1 - e^{-j\omega\tau_d}) \right|^2 \\ &= \alpha^2(1-\gamma)^2\tau_d^2 + 2\alpha^2\tau_d^2\gamma\,(1-\gamma)\cos((\tau_c - \tau_l)\omega) \\ &\quad + \tau_d^2\omega^2 - 2\tau_d^2\alpha\omega(\gamma\,\sin(\tau_l\omega) + (1-\gamma)\sin(\tau_c\omega)) \\ &\quad - 2\gamma^2(\alpha\tau_d + 1)(1 - \cos(\tau_d\omega)) > 0. \end{aligned} \tag{62}$$

Since $\cos(z) \leq 1$ integrating both sides from 0 to z yields $\sin(z) \leq z$ when $z \geq 0$ and integration again yields $1 - \cos(z) \leq z^2/2$ when $z > 0$. Therefore,

$$1 - \cos(\tau_d\omega) \leq \frac{1}{2}(\tau_d\omega)^2, \tag{63}$$

$$\cos((\tau_c - \tau_l)\omega) \geq 1 - \frac{(\tau_c - \tau_l)^2\omega^2}{2}, \tag{64}$$

$$\sin(\tau_l\omega) \leq \tau_l\omega, \quad \sin(\tau_d\omega) \leq \tau_d\omega, \quad \sin(\tau_c\omega) \leq \tau_c\omega, \tag{65}$$

since the frequency ω are positive. Substituting these inequalities into Eq. (62) yields

$$\begin{aligned} f(\omega, \gamma, \tau_c) &\geq \omega^2\tau_d^2 \Big[1 - \alpha^2\gamma\,(1-\gamma)(\tau_c - \tau_l)^2 - \gamma^2(\alpha\tau_d + 1) \\ &\quad - 2\alpha(\gamma\,\tau_l + (1-\gamma)\tau_c) \Big] + \alpha^2\tau_d^2(1-\gamma)^2 \\ &> 0, \qquad \forall\omega > 0, \end{aligned} \tag{66}$$

which is satisfied if the coefficient of the ω^2 term is positive, i.e.,

$$\begin{aligned} p(\gamma) &= 1 - \alpha^2\gamma\,(1-\gamma)(\tau_c - \tau_l)^2 - 2\alpha(\gamma\,\tau_l + (1-\gamma)\tau_c) \\ &\quad - \gamma^2(\alpha\tau_d + 1) > 0. \end{aligned} \tag{67}$$

By collecting all the time-delay terms to one side of the equation, the above inequality can be rewritten as

$$\begin{aligned} \gamma\,(1-\gamma)\left(\frac{\tau_c}{1/\alpha} - \frac{\tau_l}{1/\alpha} \right)^2 + 2\left(\gamma\,\frac{\tau_l}{1/\alpha} + (1-\gamma)\frac{\tau_c}{1/\alpha} \right) \\ + \gamma^2\left(\frac{\tau_d}{1/\alpha} \right) \qquad < \left(1 - \gamma^2 \right). \end{aligned} \tag{68}$$

Note that this inequality cannot be satisfied with the blending gain $\gamma = 1$, since the right hand side becomes zero, and the time delays and the time constant $1/\alpha$ are non-negative, which leads to the condition in Eq. (58) of the lemma. However, with $\gamma < 1$, the inequality in Eq. (68) is always satisfied provided all the delays are sufficiently small since the left hand side tends to zero. □

Lemma 4 ensures string stability if the delays are small. String stability can be numerically assessed for a given set of delay values by directly evaluating the condition on $f(\omega)$ in Eq. (62) over a finite frequency interval, as shown next.

Lemma 5: The CVS, with the blended protocol in Eq. (15) satisfying the internal stability conditions as in Remark 6,

meets the string stability condition in Eq. (17) on the error-propagation transfer function $G_i(s)$ provided the minimum value of $f(\omega)$ over the bounded interval $[0, \omega^*]$ in Eq. (62) is positive, i.e.,

$$\min_{\omega\in(0,\omega^*]} f(\omega, \gamma, \tau_c) > 0, \tag{69}$$

where

$$\omega^* = \alpha\left(1 + 2\sqrt{\frac{1}{3} + \frac{\alpha\tau_d + 1}{\alpha^2\tau_d^2}}\right). \tag{70}$$

Proof: The string stability condition $f(\omega) > 0$ in Eq. (62) is always satisfied if ω is large, as the condition can be rewritten as (since sine and cosine are bounded functions)

$$\begin{aligned} f(\omega, \gamma, \tau_c) > {} & \alpha^2(1-\gamma)^2\tau_d^2 - 2\alpha^2\tau_d^2\gamma(1-\gamma) + \tau_d^2\omega^2 \\ & - 2\tau_d^2\alpha\omega - 4\gamma^2(\alpha\tau_d + 1) \quad > 0, \end{aligned} \tag{71}$$

which is equivalent to

$$\begin{aligned} (\omega-\alpha)^2 > {} & \alpha^2(4\gamma - 3\gamma^2) + 4\frac{\gamma^2}{\tau_d^2}(\alpha\tau_d + 1), \\ \text{or } \omega > {} & \alpha\left(1 + 2\sqrt{(\gamma - \frac{3}{4}\gamma^2) + \frac{\gamma^2(\alpha\tau_d+1)}{\tau_d^2\alpha^2}}\right), \end{aligned} \tag{72}$$

and is always satisfied if $\omega > \omega^*$ in Eq. (70) since $\max_{0\le\gamma\le1}(\gamma - 3\gamma^2/4) = 1/3$ and $\gamma \le 1$. □

Remark 7 (String stability assumption): The CVS is assumed to be string stable in the rest of the article by satisfying the stability condition in Lemma 5, esp., $\gamma < 1$ from Lemma 4.

C. Steady-State Error of CVS

The proposed approach maintains constant steady-state spacing between vehicles.

Lemma 6: Constant steady-state spacing between vehicles for a desired trajectory with constant velocity is maintained with the blended protocol in Eq. (15) satisfying the internal stability conditions in Remark 6. Specifically, with desired trajectory $x_0(t) = Vt$ and

$$x_0(s) \ = v_0(s)/s \ = V/s^2 \tag{73}$$

the relative spacing error δ_i is zero, $\lim_{t\to\infty}\delta_i(t) = 0$, for all follower vehicles, i.e., $i \ge 2$.

Proof: The steady-state spacing error $\delta_i = x_{i-1} - x_i$ for each follower vehicle ($i \ge 2$) can be found from Eq.(17) as,

$$\begin{aligned} \delta_i(s) = G_{i-1}\delta_{i-1}(s) \ &= \left(\prod_{j=1}^{i-1} G_j(s)\right)\delta_1(s) \\ &= G^{i-2}(s)G_1(s)\delta_1(s) \quad \text{(using Eq. (61))} \\ &= G^{i-2}(s)G_1(s)G_0(s)v_0(s), \\ &= G^{i-2}(s)G_1(s)G_0(s)\frac{V}{s}, \end{aligned} \tag{74}$$

where

$$\begin{aligned} G_0(s) = \frac{\delta_1(s)}{v_0(s)} &= \frac{x_0(s) - x_1(s)}{sx_0(s)} = \frac{1 - T_1(s)}{s} \\ &= \frac{1}{s + \alpha e^{-s\tau}} \quad \text{(using Eqs. (23), (27), (37))}. \end{aligned} \tag{75}$$

Similarly, the transfer function $G_1(s)$ can be found from Eq. (56). The denominator of G_1 in Eq. (56) can be obtained from the expression of T_1 in Eq.(23), and G_{c0} in Eq. (27) and $D_0(s)$ in Eq. (29), with $\beta = 1$,

$$\begin{aligned} 1 - T_1(s) &= 1 - \frac{G_{c0}(s)}{D_0(s)} = 1 - \frac{\alpha e^{-s\tau_l}}{s + \alpha e^{-s\tau_l}} \\ &= \frac{s}{s + \alpha e^{-s\tau_l}} = \frac{s}{D_0(s)}. \end{aligned} \tag{76}$$

The numerator of G_1 in Eq. (56) can be found from Eq. (32), resulting in, using Eq.(23), and Eqs.(25)-(30), with $\beta = 1$,

$$\begin{aligned} & T_1(s) - T_2(s) \\ &= \left(1 - \frac{G_f(s)}{D(s)}\right)\frac{G_{c0}(s)}{D_0(s)} - \frac{G_c(s)}{D(s)} \\ &= \frac{(D(s) - G_f(s))G_{c0}(s) - G_c(s)D_0(s)}{D(s)D_0(s)} \\ &= \frac{\alpha s e^{-s\tau_l}((1-(1-\gamma)e^{-s(\tau_c-\tau_l)}) - \gamma e^{-s\tau_l}\frac{1-e^{-s\tau_d}}{s\tau_d})}{(s + \alpha e^{-s\tau_l})(s + \alpha(\gamma e^{-\tau_l} + (1-\gamma)e^{-s\tau_c}))}. \end{aligned} \tag{77}$$

Substituting Eqs. (76) and (77) into Eq. (56) yields

$$G_1(s) = \frac{\alpha e^{-s\tau_l}(1-(1-\gamma)e^{-s(\tau_c-\tau_l)} - \gamma e^{-s\tau_l}\frac{1-e^{-s\tau_d}}{s\tau_d})}{(s + \alpha(\gamma e^{-s\tau_l} + (1-\gamma)e^{-s\tau_c}))}. \tag{78}$$

The limit as s tends to zero for the error transfer functions in Eqs.(61) and (75) are given by

$$\begin{aligned} \lim_{s\to0} G(s) &= \lim_{s\to0}\frac{e^{-s\tau_l}\gamma(\alpha\tau_d + 1 - e^{-s\tau_d})}{\tau_d(s + \alpha(\gamma e^{-s\tau_l} + (1-\gamma)e^{-s\tau_c}))} \\ &= \gamma, \end{aligned} \tag{79}$$

$$\lim_{s\to0} G_0(s) = \lim_{s\to0}\frac{1}{s + \alpha e^{-s\tau_l}} = \frac{1}{\alpha}. \tag{80}$$

and from Eq. (78)

$$\begin{aligned} \lim_{s\to0} G_1(s) \ &= \lim_{s\to0}\frac{\alpha\gamma(s - e^{-s\tau_l}\frac{1-e^{-s\tau_d}}{\tau_d})}{s\alpha} \\ &= \lim_{s\to0}\frac{\alpha\gamma(s - \frac{1-e^{-s\tau_d}}{\tau_d})}{s\alpha}. \end{aligned} \tag{81}$$

Note that the Taylor expansion of $e^{-s\tau_d}$

$$e^{-s\tau_d} = 1 - \tau_d s + \frac{1}{2}(\tau_d s)^2 + \ldots, \tag{82}$$

and therefore, from Eq. (81),

$$\begin{aligned} \lim_{s\to0} G_1(s) &= \lim_{s\to0}\frac{\alpha\gamma(\frac{1}{2}\tau_d s^2 - \frac{1}{6}\tau_d^2 s^3 + \ldots)}{s\alpha} \\ &= \lim_{s\to0}\frac{\alpha\gamma(\frac{1}{2}\tau_d s - \frac{1}{6}\tau_d^2 s^2 + \ldots)}{\alpha} = 0. \end{aligned} \tag{83}$$

Finally, substituting Eqs. (79), (80) and (83) into Eq. (74), the steady state spacing error of all follower vehicles $i \ge 2$ is

$$\begin{aligned} \lim_{t\to\infty}\delta_i(t) &= \lim_{s\to0} s\delta_i(s) \\ &= \lim_{s\to0} s[G_1(s)]\left(G^{i-2}(s)G_0(s)\right)\frac{V}{s} \\ &= \lim_{s\to0}[G_1(s)]\left(G^{i-2}(s)G_0(s)\right)V = 0, \end{aligned} \tag{84}$$

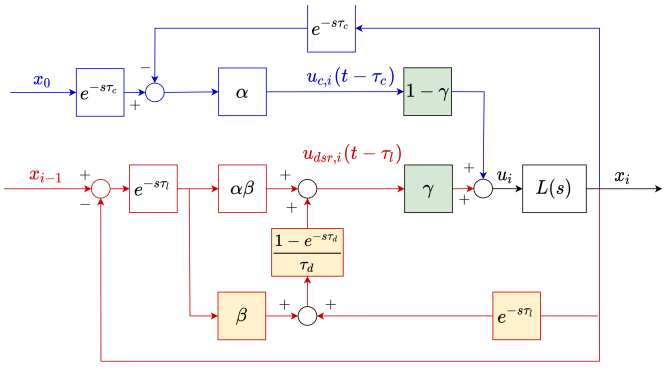

Fig. 3. The block diagram of PLF with DSR for the follower vehicles $i \geq 2$ in Eq. (22), with communication delay τ_c, local sensing delay τ_l, and DSR delay τ_d. The vehicle control $u_{c,i}$ using centralized information is depicted in blue and control $u_{dsr,i}$ using decentralized sensing is in red. The DSR augmentation of the traditional feedback is shown in yellow shaded blocks, and the blending of centralized and decentralized control is shown in green shaded blocks. When centralized communication is lost $u_{c,i}$ is set to zero. For PLF without DSR, the yellow blocks are set to zero and the green blocks are set to 1.

since the limit as s tends to zero of $G_1(s)$ is zero and the limits of $G(s) = G_i(s)$ and $G_0(s)$ are bounded, resulting in the maintaining of constant spacing by all the followers. □

D. Loss of Centralized Communication (use of DSR alone)

This subsection considers the impact when DSR alone is used due to the loss of centralized communication of the desired trajectory to the followers. Specifically, this section considers the case when the blended protocol in Eq. (15) is reduced to the purely predecessor-follower DSR case (and referred to as PF with DSR), for the followers, i.e.,

$$\begin{aligned}\dot{x}_i(t) &= \gamma\, u_{dsr}(t-\tau_l), \qquad i \geq 2\\ \dot{x}_1(t) &= \gamma\, u_{dsr,1}(t-\tau_l) + (1-\gamma)u_{c,1}(t-\tau_l)\\ &= -\alpha(x_1(t-\tau_l) - x_0(t-\tau_l)).\end{aligned} \tag{85}$$

This PF with DSR can be represented by the block diagram in Fig. 3 without the blue centralized control, i.e., $u_{c,i}(t) = 0$.

It is well known that, without centralized control, constant spacing cannot be maintained while remaining string stable. In the following, it is shown that even under full communication loss, the DSR-based approach to constant spacing platooning (i) remains internally stable (Lemma 7), and (ii) is string stable (Lemma 8). The cost of this string stability is an increase in steady state spacing error similar to standard PLF (where the steady state spacing error is proportional to the time constant $1/\alpha$ [24]), and quantified in Lemma 9. The steady state error is also shown to decrease with larger values of blending gain γ.

1) Internal Stability With DSR Alone:

Lemma 7: Internal stability is maintained if centralized communication to the followers is lost as in Eq. (85) when the local sensing delay τ_l satisfies the internal stability condition with the centralized communication in Lemmas 2 and 3, i.e., $\tau_l < \frac{\pi}{2\alpha}$, as in Eq. (53).

Proof: With loss of the centralized communication and the control as in Eq. (85), the relationship between the spacing of adjacent vehicles can be obtained from Eqs. (21), (22) with $\beta = 1$ as, for $i \geq 2$

$$x_i(s) = \frac{\gamma\, e^{-s\tau_l}}{\tau_d}\left(\frac{(1-e^{-s\tau_d}) + \alpha\tau_d}{s + \alpha\gamma\, e^{-s\tau_l}}\right) x_{i-1}(s). \tag{86}$$

From Eq. (85), the dynamics of the leader is not impacted. Therefore, the characteristic function $D_0(s)$ for the leader is the same as in Eq. (37), which requires $\tau_l < \pi/(2\alpha)$ for the internal stability of the leader. From Eq. (86), the characteristic function $D(s)$ of the dynamics of the followers are given by

$$D(s) = s + \alpha\gamma\, e^{-s\tau_l}. \tag{87}$$

The result follows using arguments similar to the proof of Lemma 2 to ensure that there are no imaginary axis crossing of the poles. □

2) String Stability With DSR Alone:

Lemma 8: String stability is maintained if centralized communication to the followers is lost as in Eq. (85) when satisfying the string stability condition $\gamma < 1$ in Eq. (58) and satisfying the internal stability conditions as in Remark 6, provided the blending gain $\gamma > 0$ is sufficiently small, i.e.,

$$0 < \gamma < \gamma^* = \frac{-\alpha\tau_l + \sqrt{\alpha^2\tau_l^2 + \alpha\tau_d + 1}}{\alpha\tau_d + 1}, \tag{88}$$

where the upper bound γ^* is less than one, $\gamma^* < 1$.

Proof: Following arguments similar to the proof of Lemma 4, string stability can be ensured if $G_i(j\omega) < 1$ for all $\omega > 0$, or if the function $f(\omega, \gamma)$ with $1-\gamma$ terms (corresponding to centralized communication) removed satisfies the $f(\omega) > 0$ condition for string stability in Eq. (62), i.e.,

$$\begin{aligned}f(\omega,\gamma) &= \tau_d^2\omega^2 - 2\tau_d^2\alpha\omega\gamma\,\sin(\tau_l\omega)\\ &\quad - 2\gamma^2(\alpha\tau_d+1)(1-\cos(\tau_d\omega))\\ &\geq \tau_d^2\omega^2 - 2\tau_d^2\alpha\omega^2\gamma\,\tau_l - \gamma^2(\alpha\tau_d+1)\tau_d^2\omega^2\\ &\qquad \text{(from Eqs. (63), (65))}\\ &= \tau_d^2\omega^2\left(1 - 2\alpha\gamma\,\tau_l - \gamma^2(\alpha\tau_d+1)\right) > 0.\end{aligned} \tag{89}$$

The above condition is always satisfied if the blending gain γ is sufficiently small. A bound on the blending gain γ can be found by noting that Eq. (89) is satisfied if the coefficient of ω^2 is positive

$$-\gamma^2(\alpha\tau_d+1) - 2\alpha\tau_l\gamma + 1 > 0, \tag{90}$$

where the maximum gain $\gamma^* \in [0,1]$ is found by

$$\begin{aligned}\gamma^* &= \arg\max_{\gamma\in[0,1]}\{-\gamma^2(\alpha\tau_d+1) - 2\alpha\tau_l\gamma + 1 = 0\}\\ &= \frac{-\alpha\tau_l + \sqrt{\alpha^2\tau_l^2 + \alpha\tau_d + 1}}{\alpha\tau_d + 1}\\ &< \frac{-\alpha\tau_l + \sqrt{\alpha^2\tau_l^2 + (\alpha\tau_d+1)^2 + 2\alpha\tau_l(\alpha\tau_d+1)}}{\alpha\tau_d+1}\\ &= \frac{-\alpha\tau_l + (\alpha\tau_l + \alpha\tau_d + 1)}{\alpha\tau_d+1} = 1,\end{aligned} \tag{91}$$

which proves the assertion in the lemma that the blending gain γ needs to be less than one for string stability when communication is lost. □

3) Steady-State Error With DSR Alone:

Lemma 9: When the communication to the followers is lost, the relative spacing error of the i^{th} vehicle at the steady state for the desired trajectory in Eq. (73), is given as

$$\lim_{s\to 0} s\delta_i(s) = \frac{V}{\alpha}\left(\frac{1}{\gamma} - 1\right). \tag{92}$$

Proof: The position transfer functions $T_1(s), T_2(s)$ can be found from Eqs. (23), (86), with $\beta = 1$ as

$$T_1(s) = \frac{\alpha e^{-s\tau_l}}{s + \alpha e^{-s\tau_l}}, \tag{93}$$

$$T_2 = \frac{\gamma e^{-s\tau_l}}{\tau_d}\left(\frac{(1 - e^{-s\tau_d}) + \alpha\tau_d}{s + \alpha\gamma e^{-s\tau_l}}\right) T_1(s). \tag{94}$$

resulting in the error transfer function from Eq. (56)

$$\begin{aligned} G_1(s) &= \frac{T_1(s) - T_2(s)}{1 - T_1(s)} \\ &= \frac{\alpha e^{-s\tau_l}(\tau_d s - \gamma e^{-s\tau_l}(1 - e^{-s\tau_d}))}{\tau_d s(s + \alpha\gamma e^{-s\tau_l})}. \end{aligned} \tag{95}$$

Additionally, the error propagation is, from Eq. (86), for $i \geq 2$,

$$\begin{aligned} G_i(s) &= \frac{x_i(s) - x_{i+1}(s)}{x_{i-1}(s) - x_i(s)} \\ &= \gamma\frac{e^{-s\tau_l}((1 - e^{-s\tau_d}) + \alpha\tau_d)}{\tau_d(s + \alpha\gamma e^{-s\tau_l})} = G(s). \end{aligned} \tag{96}$$

Therefore, substituting from Eqs. (80), (95) and (96) into Eq. (74), the relative spacing error of the i^{th} vehicle at the steady state is given as

$$\begin{aligned} \lim_{t\to\infty} \delta_i(t) &= \lim_{s\to 0} s\delta_i(s) = \lim_{s\to 0} [G_1(s)]\,(G(s))^{i-2}\,[G_0(s)]\,V \\ &= \left[\frac{1-\gamma}{\gamma}\right](1)^{i-2}\left[\frac{1}{\alpha}\right]V = \frac{V}{\alpha}\left(\frac{1}{\gamma} - 1\right). \end{aligned}$$

□

Remark 8 (Limitations of pure decentralized control): String stability and constant spacing cannot be guaranteed simultaneously when communication is lost based on Lemmas 8 and 9. The relative spacing error converges to zero only when the blending gain $\gamma = 1$ from Eq. (92). However, string stability requires a smaller blending gain $\gamma < \gamma^* < 1$ in Eq. (88).

E. PLF Without DSR

This section derives the standard first-order protocol for constant spacing platoon without DSR, develops conditions for internal stability and string stability and quantifies the steady-state error. This standard protocol for first-order constant spacing tracking, referred to as PLF without DSR, is given as

$$\begin{aligned} \dot{x}_i(t) &= u_{std,i}(t - \tau_l) + u_{c,i}(t - \tau_c), \quad \forall i \geq 2 \\ \dot{x}_1(t) &= u_{std,1}(t - \tau_l), \end{aligned} \tag{97}$$

where $u_{std,i}(t) = \alpha(x_{i-1}(t) - x_i(t))$. Similarly, when the second term in Eq. (97) for $i \geq 2$ is dropped due to communication loss, the method is referred to as PF without DSR in the followings. The PLF without DSR corresponds to the block diagram in Fig. 3 with the yellow blocks removed, $\beta = 1$, and gains of both the green blocks (γ and $1 - \gamma$) set to 1. Since the position transfer function of the standard protocol in Eq. (97) has the same general form as Eq. (24), arguments similar to the DSR case can be used to establish internal stability if the delays are small, and the ability to maintain constant spacing. To enable comparison with DSR, the condition to check for string stability is established below. In particular, using methods similar to the DSR case, the error transfer function of the PLF without DSR in Eq. (97) can be written as

$$G_i(s) = \frac{\alpha e^{-s\tau_l}}{s + \alpha(e^{-s\tau_l} + e^{-s\tau_c})} = G(s). \tag{98}$$

Combining with Eq. (17), the string stability requires

$$|G(j\omega)| = \left|\frac{\alpha e^{-j\omega\tau_l}}{j\omega + \alpha(e^{-j\omega\tau_l} + e^{-j\omega\tau_c})}\right| < 1, \ \forall\omega > 0, \tag{99}$$

which is equivalent to requiring, for $\omega > 0$,

$$\begin{aligned} f(\omega, \tau_c) &= |j\omega + \alpha(e^{-j\omega\tau_l} + e^{-j\omega\tau_c})|^2 - |\alpha e^{-j\omega\tau_l}|^2 \\ &= |j\omega + \alpha(e^{-j\omega\tau_l} + e^{-j\omega\tau_c})|^2 - \alpha^2 > 0. \end{aligned} \tag{100}$$

Lemma 10: The CVS, with the standard protocol in Eq. (97) meets the string stability condition in Eq.(17) on the error- propagation transfer function $G_i(s)$ provided the minimum value of $f(\omega)$ in Eq. (100) is positive over the bounded interval $[0, \omega^*]$, i.e. with $\omega^* = 4\alpha$,

$$\min_{\omega\in[0,\omega^*]} f(\omega, \tau_c) > 0. \tag{101}$$

Proof: The string stability condition $f(\omega) > 0$ in Eq. (100) is always satisfied for large ω, since

$$\begin{aligned} f(\omega, \tau_c) &= 2\alpha^2 + 2\alpha^2\cos((\tau_c - \tau_l)\omega) + \omega^2 \\ &\quad - 2\alpha\omega(\sin(\tau_l\omega) + \sin(\tau_c\omega)) \\ &\geq 2\alpha^2 - 2\alpha^2 + \omega^2 - 4\alpha\omega \\ &= \omega^2 - 4\alpha\omega > 0, \end{aligned} \tag{102}$$

which is equivalent to $\omega > 4\alpha = \omega^*$. □

IV. Results and Discussion

In this section, simulations with typical CVS parameters from literature, are used to illustrate the impact of control parameter selections such as blending gain γ as well as DSR gain β, and to estimate the benefits of using the proposed DSR method.

A. System Description

1) CVS Parameter Selection: The performance of PLF with DSR (Eq. (15)) is evaluated through simulations using the MATLAB/Simulink environment. The simulations include the CVS with one leader and four followers. In the following, the different methods are evaluated for a step change in the target velocity, with the platoon accelerating from static to the target velocity of $V = 20$ m/s. Except for the communication delay τ_c and the blending gain γ, the rest of the parameters are selected as typical CVS values, as discussed below.

(i) Control gain α: Depending on the types of the vehicles, the target settling time for accelerating from $V = 0$ to $V = 20$ m/s varies from $5 - 10$ s for typical automobile cruise control systems on passenger cars [25], to $10 - 30$ s for heavy duty trucks [26]. In this paper the controller gain α is selected as $\alpha = 0.4$ to match the settling time of 10 s.

(ii) Local sensing delay τ_l and DSR delay τ_d: The local sensing delay depends on the update rate of the distance sensors and the processors. Typically the local sensor delay τ_l varies between 0.1 to 0.3 s [27], [28]. In the simulations, the DSR delay τ_d is set to be the same as the local sensing delay, $\tau_d = \tau_l = 0.1$ s. It is selected the same as the update rate of the Bosch Mid Range Radar (MRR) sensor, which is widely used in vehicles with Advanced Driver Assistance Systems (ADAS) systems [29]. The controller also outputs the discrete control signal with the sampling time as $\tau_d = 0.1$ s.

2) Vehicle Model: The individual vehicle dynamics is selected as a double integrator model as in recent work, e.g., [7] $\tilde{L}_i(s) = \frac{1}{s^2}$, and according to Eqs. (3), (4), the feedback controllers $C_{ff,i}(s)$ and $C_{fb,i}(s)$ are selected as

$$C_{ff,i}(s) = s + 10\alpha, \qquad C_{fb,i}(s) = 10\alpha\ s, \tag{103}$$

with $k_1 = 10\alpha = 4$ for the feedforward controller $C_{ff,i}(s)$ to have a higher bandwidth (by a decade) compared to the velocity dynamics. Note that the choice of $k_1 = 4$ also ensures that the canceled pole $s = -4$ is stable [30]. For real-time simulations, the controller does not have direct access to the derivative of the relative spacing through local sensing. Therefore, a low-pass filter with cutoff frequency $\omega_f = 40\alpha = 16$ rad/s is added to prevent the amplification of the high frequency noise during computations of the derivative [31], which results in a modified feedforward controller $C_{ff,i}(s) = \frac{\omega_f}{(s+\omega_f)}(s + 10\alpha)$.

3) Metrics: To evaluate the convergence speed to steady-state, the settling time T_s of the CVS is defined as the minimum time required for the states of all the vehicles to settle and remain within 2% of the final steady-state values. Besides, in order to evaluate the ability to maintain constant-spacing during the transient process, the maximum deviation δ_m of the CVS is defined by

$$\delta_m = \max_{t\geq 0} \|X(t) - x_0(t)\mathbf{1}_n\|_\infty, \tag{104}$$

where the vector $\mathbf{1}_n = [1, \ldots, 1] \in \mathbb{R}^n$. The step response is selected as the source signal for computing the settling time and comparing the spacing error response.

B. Impact of Varying the Blending Gain γ

The impact of increasing the blending gain γ, i.e., more reliance on local sensing than the centralized command, on internal and string stability as well as performance are investigated to guide the selection of the blending gain γ.

1) Internal Stability: Selecting larger values for the blending gain γ reduces the reliance on the centralized command, and therefore, increases the acceptable communication delay τ_c for internal stability. For example, the acceptable communication delay for internal stability is given as $\tau_c < \pi/(2\alpha) \approx 3.92$ s according to Lemma. 2. However, increasing the blending gain γ such that $\gamma > \frac{1}{1+\cos(\tau_l\alpha)} \approx 0.50$, ensures internal stability regardless of the communication delay τ_c, according to Lemma 3, and indicated in Fig. 4.

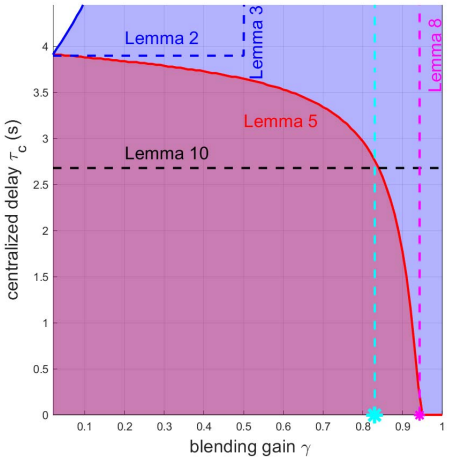

Fig. 4. For comparative evaluations, the blending gain γ for PLF with DSR is selected (vertical cyan dashed line) to achieve the same acceptable communication delay τ_c^* as PLF without DSR (horizontal black dashed line) for string stability found from Eq. (106), Lemma 10. The vertical purple dashed line marks the maximum acceptable blending gain γ^* from Eq. (107), Lemma 8. The string-stable region (the red shaded area) is computed from Eq. (105), Lemma 5. The internally-stable region (the blue shaded area) is found numerically by checking for finite settling time of the step response using MATLAB and can be estimated by Lemmas 2 and 3.

2) String Stability: Selecting larger values for the blended gain γ, i.e., smaller amount of centralized command reduces the acceptable communication delay τ_c for string stability, as shown in Fig. 4. This is expected since sufficient centralized command is needed to make constant-spacing PLF string stable, and pure decentralized DSR ($\gamma = 1$) cannot maintain string stability, according to Remark 8.

Given a target acceptable communication delay τ_c^* for string stability, the candidate set of all the available blending gain S_γ can be solved numerically via the following expression, according to Lemma 5,

$$\begin{aligned} S_\gamma &= \{\gamma \in [0,1] \mid \min_{\omega\in(0,\omega^*]} f(\omega, \gamma, \tau_c^*) > 0\}, \\ \omega^* &= \alpha\left(1 + 2\sqrt{650.3}\right) = 20.80 \text{ rad/s}, \end{aligned} \tag{105}$$

with $f(\omega, \gamma, \tau_c)$ defined in Eq. (62). The range of the candidate set S_γ reduces as the communication delay τ_c increases, as indicated in the red shaded area in Fig. 4.

3) Selection of Blending Gain: The blending gain γ is selected so that the acceptable communication delay τ_c^* for string stability is the same for PLF, with and without DSR. For PLF without DSR, the acceptable communication delay τ_c^* for string stability can be solved numerically via the following expression, according to Lemma 10,

$$\tau_c^* = \sup_{\tau_c>0} \min_{\omega\in(0,\omega^*]} f(\omega, \tau_c) > 0, \quad \omega^* = 4\alpha = 1.6 \text{ rad/s}, \tag{106}$$

with $f(\omega, \tau_c)$ in Eq. (100). From Eq. (106), the acceptable communication delay for string stability is solved as $\tau_c^* = 2.68$ s. To achieve the same acceptable communication delay

for PLF with DSR, the candidate set S_γ can be solved as $0 \leq \gamma \leq 0.83$ numerically by substituting $\tau_c^* = 2.68$ s into Eq. (105). The largest value of $\gamma = 0.83$ is selected for PLF with DSR since this selection reduces the steady-state error when the communication is lost, according to Lemma 9. Lastly, choosing $\gamma = 0.83$ guarantees string stability when the communication is lost, according to Lemma 8,

$$\gamma = 0.83 < \gamma^* = \frac{-\alpha\tau_l + \sqrt{\alpha^2\tau_l^2 + \alpha\tau_d + 1}}{\alpha\tau_d + 1} = 0.94, \tag{107}$$

where the upper bound $\gamma^* = 0.94$ is computed from Eq. (88).

C. Robustness to Communication Delay

Simulations are used to demonstrate that the use of DSR improves CVS performance, with robustness to large communication delays. Moreover, it is shown that the spacing error is reduced substantially by use of DSR when communication is lost.

1) Typical Communication Delay Case: The proposed PLF with DSR enables both string stability and constant spacing, similar to the PLF without DSR in the presence of typical communication delays. In particular, with a communication delay of $\tau_c = 0.5$ s [7], [12], the maximum deviation δ_m for the PLF with DSR during the transition is 2.37 m, compared to the maximum deviation $\delta_m = 2.77$ m for the PLF without DSR. The maximum spacing errors during transients in both cases are less than 10 m, which is typically acceptable for CSP CVS systems in literature, e.g., [13]. The settling time T_s for both methods are 9.4s, which achieves the target settling time of 10s. Therefore, both, PLF with DSR and PLF without DSR have acceptable performance under typical communication delays.

2) Large Communication Delay Case: The PLF with DSR has more robust performance to large communication delays, i.e., maintains constant steady-state spacing with similar convergence rate and the maximum transient deviation as the typical-communication delay case. In contrast, the PLF without DSR results in substantial increase in the settling time T_s and the maximum deviation δ_m as the communication delay τ_c increases. The settling time T_s for the PLF with DSR approach changes from 9.4 s ($\tau_c = 0.1$ s) to 10.7 s ($\tau_c = 2.5$ s), as seen in Fig. 6(a). In contrast, for the PLF without DSR, the settling time T_s changes from 9.4 s ($\tau_c = 0.1$ s) to 35.5 s ($\tau_c = 2.5$ s), as seen in Fig. 6(b). Therefore, the variation of the settling time with DSR (1.3 s) is about 95% less than the variation of the settling time without DSR (26.1 s). Furthermore, the maximum transient deviation δ_m of the PLF with DSR is 4.69 m, which is 74.05% less than the maximum transient deviation $\delta_m = 18.11$ m of the PLF without DSR, as seen in Fig. 6(a), (b). Therefore, the tracking performance of the proposed PLF with DSR approach is more robust to large centralized delay compared with the PLF without DSR.

3) Communication Loss Case: When communication is lost, the proposed PF with DSR has better tracking performance compared to PF without DSR. The maximum deviation δ_m with DSR approach is 10.22 m, which is an increase

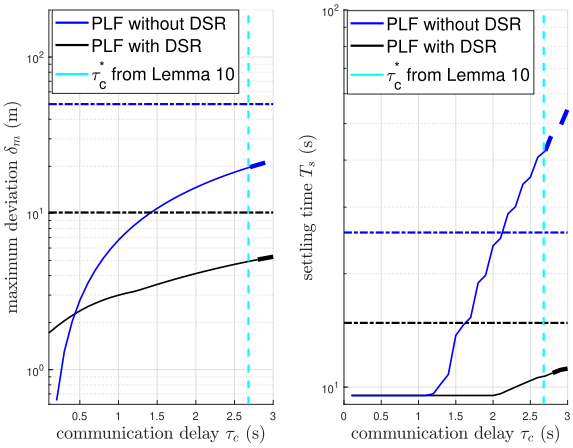

Fig. 5. Comparison of maximum deviation δ_m (left plots) and settling time T_s (right plots) for PLF with DSR (black lines) and PLF without DSR (blue lines) as communication delay increases till string instability (vertical cyan lines). Horizontal dashed lines represent communication loss case. Left: With communication loss, PLF with DSR has less steady state spacing error δ_m (horizontal black line) than PLF without DSR (horizontal blue line). Right: Settling time T_s variation with communication delay is substantially smaller with DSR compared to the case without DSR.

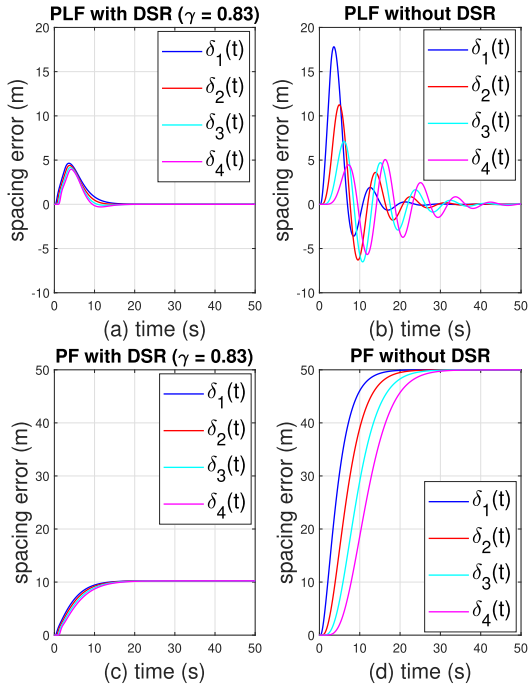

Fig. 6. DSR (left plots) leads to more cohesive tracking performance and smaller spacing errors δ_i when compared to the case without DSR (right plots) under large communication delays $\tau_c = 2.5$ s (top plots) or communication loss (bottom plots).

of about 0.5 s headway time, as seen in Fig. 6(c). This numerically obtained value of 10.22 m is also close to the predicted steady-state error from Eq. (92) in Lemma 9 given by

$$\lim_{s\to 0} s\delta_i(s) = \frac{V}{\alpha}\left(\frac{1}{\gamma} - 1\right) = \frac{20}{0.4}\left(\frac{1}{0.83} - 1\right) = 10.24.$$

In contrast, with communication loss, the maximum deviation δ_m is 50 m without DSR, which is about 2.5 s headway time, as seen in Fig. 6(d). The speed-dependent spacing error with

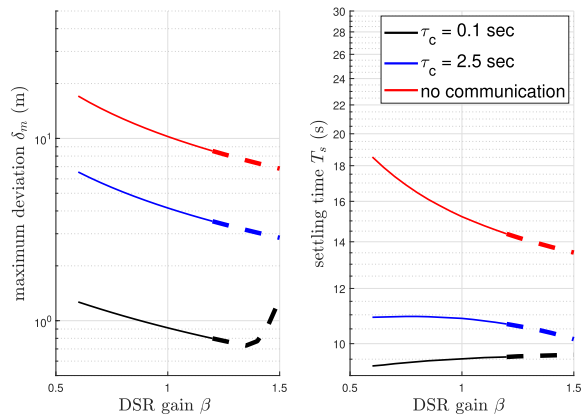

Fig. 7. Impact of the DSR gain β on the maximum deviation δ_m (left plots) and settling time T_s (right plots) under small communication delay (black lines), large communication delay (blue lines) and communication loss (red lines). Dashed line indicates when the CVS is string unstable. Increasing the DSR gain β can improve the performance, but can also make the system string unstable.

DSR (10.22m) is about 80% less than the speed-dependent spacing error without DSR (50 m). Thus, the PF with DSR is able to maintain small inter-vehicle spacing in the platoon even without communication.

D. Impact of Varying DSR Gain β

The impact of varying the DSR gain β on the CVS performance is shown in Fig. 7 for different communication delay conditions. Overall, the performance of the proposed DSR approach can be improved further by increasing the DSR gain, i.e., when $\beta > 1$. However, the CVS can also become string unstable with larger DSR gain β, as seen in Fig. 7. In particular, when the communication delay is small ($\tau_c = 0.1$ s), the maximum deviation δ_m can be further reduced to 0.80 m (with $\beta = 1.2$) from $\delta_m = 0.91$ m when $\beta = 1$. However, the settling time T_s increases as DSR gain β increases beyond one. When the communication delay is large ($\tau_c = 2.5$ s), the maximum deviation δ_m can be further reduced to 3.51 m ($\beta = 1.2$) from $\delta_m = 4.15$ m ($\beta = 1$) and the settling time T_s can be further reduced as well to 10.67 s ($\beta = 1.2$) from with $T_s = 10.87$ s ($\beta = 1$). The results are similar when communication is lost. The maximum deviation δ_m can be further reduced to 8.53 m ($\beta = 1.2$) from $\delta_m = 10.24$ m ($\beta = 1$). The settling time T_s can be further reduced to 14.37 s, compared with $T_s = 15.21$ s ($\beta = 1$). In all cases, the maximum deviation δ_m improves (by upto 20%) with increasing DSR gain β, but the improvement is limited by the advent of string instability as shown in Fig. 7.

V. Conclusion

This work addressed the constant-spacing platooning problem in the presence of large communication delays and loss of communication. Centralized control from the lead vehicle was blended with a new delayed-self-reinforcement (DSR) approach that mimics the ideal centralized control in a decentralized manner. As a result, the DSR-based approach improved performance in the presence of large communication delays as well as communication loss. The article developed conditions for maintaining internal stability, string stability and constant spacing without steady-state error for the proposed blended DSR approach. Simulation results showed that the tracking performance of predecessor-leader following was more robust to large communication delays and loss with the proposed DSR approach when compared to the case without DSR.

References

[1] D. Swaroop and J. K. Hedrick, "Constant spacing strategies for platooning in automated highway systems," *J. Dyn. Syst. Meas. Control*, vol. 121, no. 3, pp. 462–470, 1999.
[2] A. Alam, B. Besselink, V. Turri, J. Mårtensson, and K. H. Johansson, "Heavy-duty vehicle platooning for sustainable freight transportation: A cooperative method to enhance safety and efficiency," *IEEE Control Syst. Mag.*, vol. 35, no. 6, pp. 34–56, Dec. 2015.
[3] S. E. Li et al., "Dynamical modeling and distributed control of connected and automated vehicles: Challenges and opportunities," *IEEE Intell. Transp. Syst. Mag.*, vol. 9, no. 3, pp. 46–58, Jul. 2017.
[4] P. Seiler, A. Pant, and K. Hedrick, "Disturbance propagation in vehicle strings," *IEEE Trans. Autom. Control*, vol. 49, no. 10, pp. 1835–1842, Oct. 2004.
[5] P. A. Ioannou and C. C. Chien, "Autonomous intelligent cruise control," *IEEE Trans. Veh. Technol.*, vol. 42, no. 4, pp. 657–672, Nov. 1993.
[6] L. Cui, Z. Chen, A. Wang, J. Hu, and B. B. Park, "Development of a robust cooperative adaptive cruise control with dynamic topology," *IEEE Trans. Intell. Transp. Syst.*, vol. 23, no. 5, pp. 1–12, May 2021.
[7] Y. G. Liu, H. L. Gao, C. J. Zhai, and W. Xie, "Internal stability and string stability of connected vehicle systems with time delays," *IEEE Trans. Intell. Transp. Syst.*, vol. 22, no. 10, pp. 6162–6174, Oct. 2021.
[8] X. Liu, A. Goldsmith, S. Mahal, and J. Hedrick, "Effects of communication delay on string stability in vehicle platoons," in *Proc. IEEE Intell. Transp. Syst.*, Aug. 2001, pp. 625–630.
[9] M. Boban and P. M. D'Orey, "Exploring the practical limits of cooperative awareness in vehicular communications," *IEEE Trans. Veh. Technol.*, vol. 65, no. 6, pp. 3904–3916, Jun. 2016.
[10] J. Karedal, N. Czink, A. Paier, F. Tufvesson, and A. F. Molisch, "Path loss modeling for vehicle-to-vehicle communications," *IEEE Trans. Veh. Technol.*, vol. 60, no. 1, pp. 323–328, Jan. 2011.
[11] B. Tian, X. Deng, Z. Xu, Y. Zhang, and X. Zhao, "Modeling and numerical analysis on communication delay boundary for CACC string stability," *IEEE Access*, vol. 7, pp. 168870–168884, 2019.
[12] Y. Zhang, Y. Bai, M. Wang, and J. Hu, "Cooperative adaptive cruise control with robustness against communication delay: An approach in the space domain," *IEEE Trans. Intell. Transp. Syst.*, vol. 22, no. 9, pp. 5496–5507, Sep. 2021.
[13] Y. Li, C. Tang, S. Peeta, and Y. Wang, "Nonlinear consensus-based connected vehicle platoon control incorporating car-following interactions and heterogeneous time delays," *IEEE Trans. Intell. Transp. Syst.*, vol. 20, no. 6, pp. 2209–2219, Jun. 2019.
[14] J. Ploeg, E. Semsar-Kazerooni, G. Lijster, N. van de Wouw, and H. Nijmeijer, "Graceful degradation of cooperative adaptive cruise control," *IEEE Trans. Intell. Transp. Syst.*, vol. 16, no. 1, pp. 488–497, Feb. 2015.
[15] C. Wu, Y. Lin, and A. Eskandarian, "Cooperative adaptive cruise control with adaptive Kalman filter subject to temporary communication loss," *IEEE Access*, vol. 7, pp. 93558–93568, 2019.
[16] J. Sawant, U. Chaskar, and D. Ginoya, "Robust control of cooperative adaptive cruise control in the absence of information about preceding vehicle acceleration," *IEEE Trans. Intell. Transp. Syst.*, vol. 22, no. 9, pp. 5589–5598, Sep. 2021.
[17] S. Devasia, "Cohesive networks using delayed self reinforcement," *Automatica*, vol. 112, Feb. 2020, Art. no. 108699.
[18] A. Bidram, F. L. Lewis, and A. Davoudi, "Synchronization of nonlinear heterogeneous cooperative systems using input–output feedback linearization," *Automatica*, vol. 50, no. 10, pp. 2578–2585, Oct. 2014.
[19] L. Zhang, J. Sun, and G. Orosz, "Hierarchical design of connected cruise control in the presence of information delays and uncertain vehicle dynamics," *IEEE Trans. Control Syst. Technol.*, vol. 26, no. 1, pp. 139–150, Jan. 2018.
[20] W. T. Tuttle, *Graph Theory*. Cambridge, U.K.: Cambridge Univ. Press, 2001.

[21] F. Jameel, M. A. Javed, and D. T. Ngo, "Performance analysis of cooperative V2V and V2I communications under correlated fading," *IEEE Trans. Intell. Transp. Syst.*, vol. 21, no. 8, pp. 3476–3484, Aug. 2020.
[22] F. L. Lewis, H. Zhang, K. Hengster-Movric, and A. Das, *Cooperative Control of Multi-Agent Systems: Optimal and Adaptive Design Approaches*. Berlin, Germany: Springer, 2013.
[23] T. Insperger and G. Stépán, *Semi-Discretization for Time-Delay Systems: Stability and Engineering Applications*, vol. 178. Berlin, Germany: Springer, 2011.
[24] W. S. Levine, *The Control Handbook*, vol. 3. Boca Raton, FL, USA: CRC Press, 2018.
[25] V. Milanés, S. E. Shladover, J. Spring, C. Nowakowski, H. Kawazoe, and M. Nakamura, "Cooperative adaptive cruise control in real traffic situations," *IEEE Trans. Intell. Transp. Syst.*, vol. 15, no. 1, pp. 296–305, Feb. 2013.
[26] J. Zhang and P. A. Ioannou, "Longitudinal control of heavy trucks in mixed traffic: Environmental and fuel economy considerations," *IEEE Trans. Intell. Transp. Syst.*, vol. 7, no. 1, pp. 92–104, Mar. 2006.
[27] M. Wang, S. P. Hoogendoorn, W. Daamen, B. van Arem, B. Shyrokau, and R. Happee, "Delay-compensating strategy to enhance string stability of adaptive cruise controlled vehicles," *Transportmetrica B, Trans. Dyn.*, vol. 6, no. 3, pp. 211–229, 2016.
[28] L. Xiao and F. Gao, "Practical string stability of platoon of adaptive cruise control vehicles," *IEEE Trans. Intell. Transp. Syst.*, vol. 12, no. 4, pp. 1184–1194, Dec. 2011.
[29] J. Hasch, "Driving towards 2020: Automotive radar technology trends," in *IEEE MTT-S Int. Microw. Symp. Dig.*, Sep. 2015, pp. 1–4.
[30] R. D. Braatz, "On internal stability and unstable pole-zero cancellations [feedback]," *IEEE Control Syst.*, vol. 32, no. 5, pp. 15–16, Oct. 2012.
[31] G. J. Naus, R. P. Vugts, J. Ploeg, M. J. van De Molengraft, and M. Steinbuch, "String-stable CACC design and experimental validation: A frequency-domain approach," *IEEE Trans. Veh. Technol.*, vol. 59, no. 9, pp. 4268–4279, Mar. 2010.

Yudong Lin received the B.Tech. degree in aerospace engineering from the Beijing Institute of Technology, Beijing, China, in 2016. He is currently pursuing the Ph.D. degree with the Mechanical Engineering Department, University of Washington, Seattle, WA, USA. His current research interests include consensus of multi-agent systems and control of vehicle networks.

Anuj Tiwari received the B.Tech. degree in civil engineering from the Indian Institute of Technology, Guwahati, India, in 2017, and the Ph.D. degree from the Mechanical Engineering Department, University of Washington, Seattle, WA, USA, in 2022. His current research interests include consensus and coordination in networked dynamical systems using a control theoretic approach with applications in connected vehicles and smart manufacturing systems.

Brian Fabien received the B.E. degree (Hons.) from The City College of New York, the M.S. degree in mechanical engineering, and the Ph.D. degree in master of philosophy from Columbia University, New York. He is a Professor of mechanical engineering, an expert in Dynamic Systems Modeling, and also worked in the Private Sector. Before being appointed the Dean with the Shiley School of Engineering, he served as an Associate Dean for academic affairs at the College of Engineering, University of Washington. Prior to his arrival in the University of Washington in 1993, he held Professorships at the University of the West Indies and Ohio University. A corporate career in engineering preceded academia, highlighted by his role as the lead mechanical engineer overseeing the guidance sensors for the famed Hubble Space Telescope. Other industry posts include Xerox Corporation, PerkinElmer, and Textron, Inc. (Lycoming Engines Division).

Santosh Devasia (Fellow, IEEE) received the B.Tech. degree (Hons.) from the Indian Institute of Technology, Kharagpur, India, in 1988, and the M.S. and Ph.D. degrees in mechanical engineering from the University of California at Santa Barbara in 1990 and 1993, respectively. He is currently a Professor of mechanical engineering at the University of Washington, Seattle, WA, USA, where he joined in 2000. He is the Director of the Boeing Advanced Research Center, University of Washington, which focuses on the manufacturing and assembly of aircraft and spacecraft structures (https://depts.washington.edu/barc/). His current research interests include iterative learning, distributed systems, and applications in human–machine interaction, manufacturing, and robotics. He is a fellow of ASME. More information can be found at: http://faculty.washington.edu/devasia/. His CODE Ocean link:/code/Platoon_Simulation.m can be found at https://codeocean.com/capsule/7706844/tree.